Proceeding of the IEEE
International Conference on Robotics and Biomimetics
Dali, China, December 2019

Magnetically Driven Wireless Capsule Robot with Targeting Biopsy Function

Dongxu Ye[1], Fan Zhang[1], Sishen Yuan[1], Shuang Song[1]*, Max Q.-H.Meng[2], *Fellow, IEEE*

***Abstract*—In this work, we present a novel magnetically actuated wireless capsule robot with biopsy function based on the principle of magnetic torsion spring (MTS). MTS is a simple device consisting of two ring-shape permanent magnets inside the capsule. It can be remotely controlled by an external uniform magnetic field so that the biopsy tool can be extended from the capsule to perform biopsy sampling operations. The energy required for biopsy is all provided by the external magnetic driving system without the need to consume the battery energy of the capsule itself. Magnetic finite element analysis is conducted to design MTS. Kinematics and force analysis of the biopsy tools is also provided. Finally, a pill-shape prototype of capsule robot is manufactured with dimension of 14 mm in diameter and 32 mm in length. In vitro experiments were carried out with this prototype to verify the feasibility of the biopsy module mechanism design and to test the ability for active locomotion.**

***Index Terms*—wireless capsule robot, biopsy module, magnetic actuation, active locomotion.**

I. Introduction

The wireless capsule endoscope (WCE) is a clinical medical examination method widely used in the human digestive tract since 2000 [1]. The main function of WCE is to take detailed images of the gastrointestinal tract for doctor diagnosis. However, with the popularity of the WCE, the traditional image capture function of WCE has been difficult to meet clinical needs. For example, when the physician is not sure whether the area being photographed is a lesion, an additional biopsy sampling is required using a flexible endoscope. This not only makes the patient very uncomfortable, but also difficult to reach the deep digestive tract area such as the small intestine. Therefore, a capsule endoscope with biopsy function has very important clinical application significance.

In order to implement the biopsy sampling function, it is necessary to provide driving force to the biopsy module. The most direct way is to use a stepper motor [2]. However, this method does not consider the energy and space consumption of the motor, so it is difficult to actually manufacture.

This work was supported in part by National Key R&D Program of China (2018YFB1307700), in part by National Natural Science Foundation of China (61803123), and in part by the Science and Technology Innovation Committee of Shenzhen(JCYJ20170413110250667).

[1]Dongxu Ye,Fan Zhang,Sishen Yuan, Shuang Song are with School of Mechanical Engineering and Automation, Harbin Institute of Technology(Shenzhen), Shenzhen, China, 518055.

[2] Max Q.-H. Meng is with Department of Electronic Engineering, the Chinese University of Hong Kong, Hong Kong, China, and affiliated with the State Key Laboratory of Robotics and Systems (HIT), Harbin Institute of Technology, China.

*Corresponding author: Shuang Song, mail: songshuang@hit.edu.cn

Sunkil Park et al. uses a shape memory alloy to trigger a torsion spring device. The biopsy module can be driven by the spring restoring force when the device is triggered [3]. Xingzhou Du et al. successfully sampled the mucus of the human small intestine by a suction force generated by a soft vacuum chamber inside the WCE [4]. The common disadvantage of these methods is that the biopsy module can only run once, and a second attempt cannot be made if the first biopsy fails.

Magnetic driving method is believed to be the most commonly used method to power the biopsy module and has been applied in many studies. For instance, Massimiliano Simi et al. completed the sampling experiment in the small intestine using magnetic torsion spring (MTS) [5]. Donghoon Son et al. controlled a small magnet in WCE to drive a fine needle to achieve reciprocating motion. Then the deep tissue of tumor can be collected by utilize the capillary effect of the fine needle [6]. Manh Cuong Hoang et al. realized multiple sampling by controlling the rotation of a single magnet to drive the biopsy tool with four blades [7]. The advantage of the magnetic driving method over other methods is that it can be powered by an external magnetic driving system. Therefore, this method does not need to consume the battery power of the WCE. In addition to power the biopsy module, the magnetic driving method can also be used to achieve the activate locomotion of the WCE. The uniform magnetic field combined with the gradient magnetic field allows the WCE realize 3-D locomotion and steering [8], hence the WCE can be actively controlled to reach any desired location in the digestive tract for a biopsy.

All sum up, we designed a novel magnetic-driven capsule robot with biopsy function in this paper. The proposed capsule introduces the principle of MTS, which consists of two ring-shape permanent magnets inside the capsule. It can be seen as a driving device. Fig.1(a) is a schematic diagram of the capsule robot working in the stomach. When an external uniform magnetic field is applied, the MTS can be used to drive the biopsy tool out of the capsule to complete the biopsy operation. The biopsy movement does not require any energy from the capsule's own battery. Thereby ensuring the functions of other modules in the capsule that require power consumption are not affected. In addition, capsules using the MTS device can be compact in size through appropriate design. This is important for micro-robot design, which is very demanding in size.

978-1-7281-6321-5/19//$31.00 ©2019 IEEE

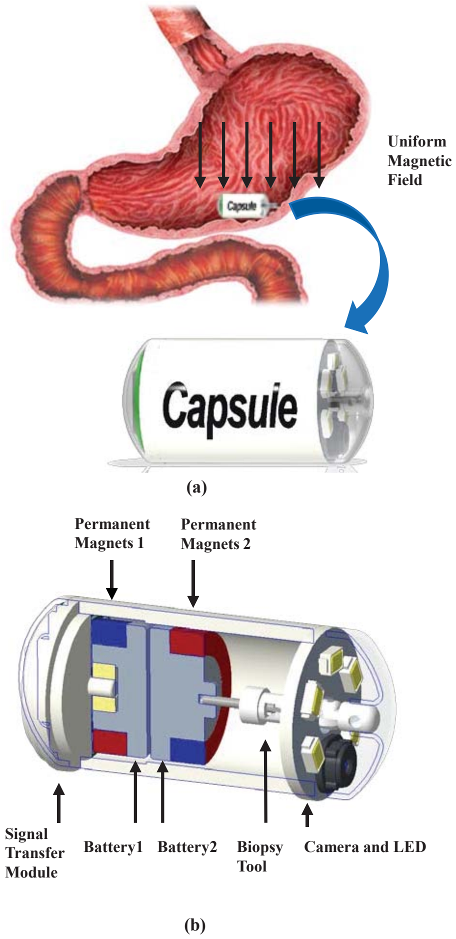

Fig. 1. Schematic diagram of the proposed capsule robot working in the stomach.(a) The biopsy module of the capsule is activated when an uniform magnetic field is applied. (b)The main structure of the capsule.

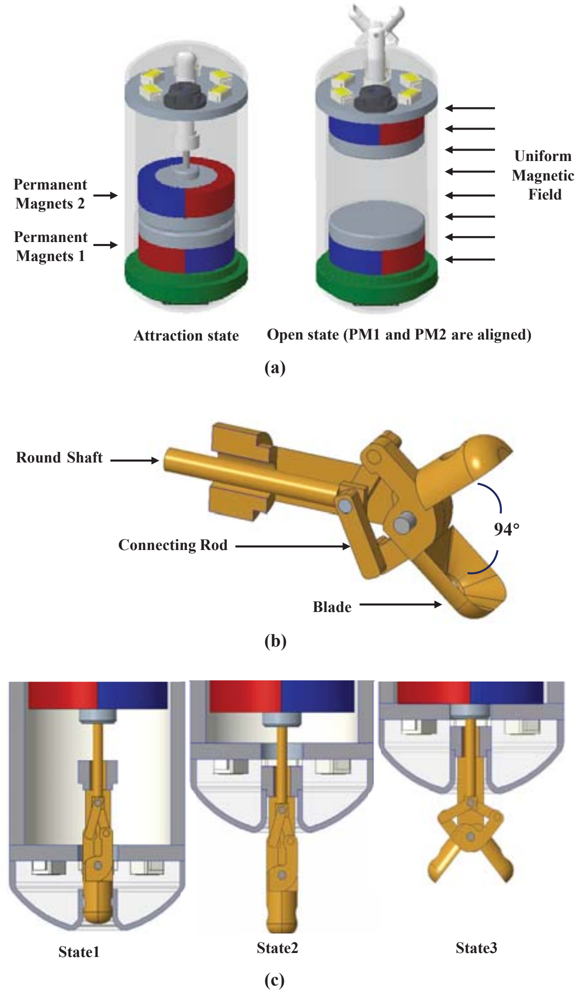

Fig. 2. Mechanism schematic of the proposed capsule robot. (a) Schematic diagram of MTS. (b) The head of a medical biopsy forceps. (c) Movement of the biopsy tool.

Structure of this paper is organized as follow: Capsule design and prototype manufacturing will be shown in Section II. The construction of the magnetic driving system for the capsule and the process and results of the experiment will be described in Section III. Finally, conclusions will be drawn in Section IV.

II. Design

A. Biopsy Module Design

Fig.1(b) shows a sectional view of the proposed capsule robot along the symmetrical plane. The conceptual design of the capsule should consist of a signal transfer module, two special-shaped batteries, a biopsy tool, a camera and LED module and two ring-shape permanent magnets (PM). Both PM are radially magnetized. PM1 is placed on battery1, which is fixed by the bearing. Therefore, PM1 can only perform a rotary motion. PM2 is placed on battery2, and a clearance fit is used between PM2 and the outer casing. As a result, PM2 is free to rotate and move in the axial direction.

The MTS composed of PM1 and PM2 is an important component of biopsy module and can be used to drive biopsy tools. MTS is a very reliable structure. In addition to the biopsy module [5], it is also widely used in the anchoring module [9] [10]of WCE. As shown in Fig.2(a), MTS is usually in the attraction state. When an external uniform magnetic field in a certain direction is applied, both the PMs will align to the external magnetic field due to the action of the magnetic moment. Then the attractive force between the two PMs will turns into a repulsive force. PM2 will move along the axial direction due to the repulsive force. The linear motion of PM2 is used to push the biopsy tool out. As soon as the external magnetic field is removed, the MTS will return to the attraction state. In addition, if the applied uniform magnetic field is rotating, the capsule will rotate accordingly, so that the biopsy forceps can point in the desired direction.

Another important component of the biopsy module is the biopsy tool. As illustrated in Fig.1(b), the biopsy tool is fixed on battery2. When MTS begins to produce repulsive force, battery2 pushes the biopsy tool out from the center of the capsule's head. This is significantly different from other capsules with biopsy function. At present, most of the other capsule's biopsy tools are extending from the side. And that creates a tricky problem because their front view cameras are not able to monitor the biopsy process. Viet Ha Le et al. addressed this problem with a side view camera [11]. However, it is difficult for a side view camera to obtain a complete image of a narrow intestine. In order to solve the problem better, we use a front view camera while extending the biopsy tool forward. This allows the operator to monitor the entire biopsy process for more accurate biopsy procedures. Meanwhile, it ensures that the camera can obtain a complete image of a narrow intestine.

The detailed structure of the biopsy tool is shown in Fig.2(b). It is the head of a medical biopsy forceps consisting of a round shaft, two connecting rods and two blades. The edge of the blade is sharp enough to cut the target tissue. When fully opened, the angle between the two blades is about 94°. As illustrated in Fig.2(c), the movement of the biopsy forceps is divided into three parts. State1 is the initial state. When the proposed capsule roboot is applied with a uniform magnetic field, the PM2 starts to drive the biopsy forceps forward. After reaching state 2, the whole body of biopsy forceps can no longer move on. From state 2 to state 3, PM2 continues to drive the round shaft to move forward. The round shaft drives the blade through the connecting rod until it is fully opened. From state 1 to state 3, PM2 has to move a total of 9mm (state1∼ state2: 7mm,state2∼ state3: 2mm). The movement of the biopsy forceps when returning is similar and will not be described here.

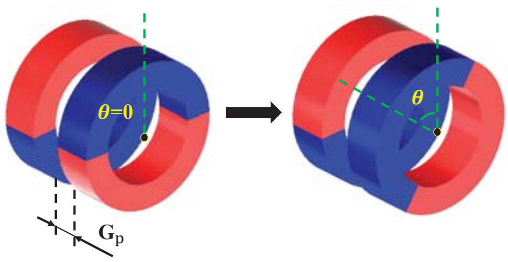

(a) (b)

Fig. 3. Schematic diagram of angular displacement of the two PMs. (a) At angular position θ=0. (b) At any angular position θ.

B. Finite Element Analysis of MTS

The first step in the analysis flow consisted in selecting the permanent magnets for the MTS. For easy swallowing, the size of the WCE should be as small as possible. At present, the size of mainstream commercial capsules is usually 11∼13mm in diameter and 24∼32mm in length [12]. Taking these size constraints into consideration, we chose a pair of ring-shape PMs with an outer diameter of 11 mm, an inner diameter of 7.2 mm, and a thickness of 3 mm. The PM were made of

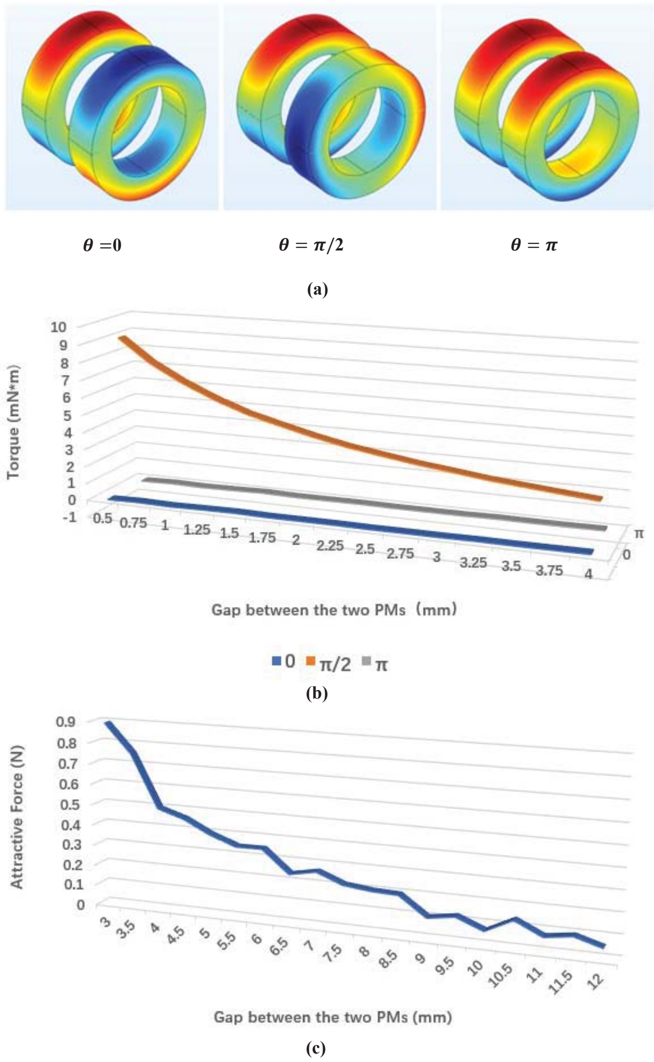

Fig. 4. Finite element simulation of MTS. (Both PM are radial magnetization, Maximum element size 0.5mm, B_r = 1.27 T, μ_r= 1.05). (a) Simulation diagram of the two PMs at different angles. Red represents the N-pole and blue represents the S-pole. (b) Torque values of PM at different angles and different gaps. (c) Attractive force of PM at different gaps.

NdFeB of which grade is N40M (B_r= 1.27 T, μ_r= 1.05). This material is the strongest magnet material we can find, and it still guarantees a relatively strong magnetic field intencity in the small volume.

When an uniform magnetic field is applied, a relative rotational motion occurs between the two PMs. We define θ as the relative displacement angle between the two PMs. As shown in Fig.3(a), when the two PMs are in the attraction state, the angular displacement θ=0. After the two PMs are aligned, θ will reach to π. During the rotation from 0 to π, torque is generated between the two PMs. The applied uniform magnetic field must be large enough to overcome the torque to align the two PMs. The torque transfer function [13] of the two PMs can be described as follows:

$$T_n(\theta) = T_g \cdot \sin\theta \tag{1}$$

where T_n represents the torque required to rotate PM from 0 to any angle θ, T_g represents the greatest torque. As shown in Fig3(a), the value of T_g is related to the gap G_p between the two PMs. In addition, T_g also depends on the parameters of PM (size, shape and magnetization direction). From Equation (1), we found that when θ=0 or π, the value of T_n is 0, and when θ=π/2, T_n reaches the maximum value which is T_g.

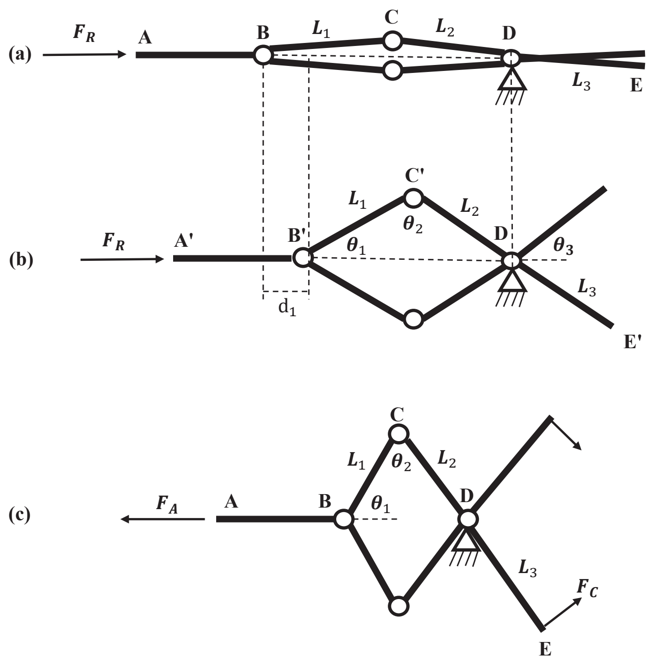

Fig. 5. Simplified schematic diagram of biopsy forceps mechanism. (a) The initial state (b) The biopsy forceps gradually open when subjected to the repulsive force F_R (d) The biopsy forceps will produce a clamping force F_C when subjected to the attractive force F_A.

Since PM's parameters have been determined, the value of T_g is now only related to the gap G_p. In order to figure out the relationship between T_g and G_p, COMSOL Multiphysics 5.4 was used for finite element analysis (FEA). The validity of the FEA approach has been demonstrated in [5] [9] [10]. As illustrated in Fig.4(a), we performed FEA for θ=0, π/2, and π cases. The value of G_p ranges from 0.5 to 4 mm, with an interval of 0.25 mm. The result of FEA is shown in Fig.4(b). As can be seen from the figure, the torque reaches the maximum value T_g when θ=π/2, and the simulation torque value tends to 0 when θ=0 or π, which is consistent with the result of Equation (1). In addition, as G_p increases, the value of T_g decreases. This means that G_p and T_g are inversely related. Since the two PMs have a minimum G_p value when they are in the attraction state, the torque T_g that needs to be overcome at this time is the largest. Considering the capabilities of our magnetic driving system, the minimum G_p=3mm is an ideal choice. This allows us to use a relatively small uniform magnetic field and ensures that the MTS can be opened remotely by our magnetic driving system.

As the driving force of the biopsy forceps, we also performed FEA on the attractive force of the two PMs. The angle θ between the two PMs is fixed at 0, at which position they produce the peak attractive force. As mentioned before, the minimum G_p is 3 mm, and the PM2 needs to move 9 mm to fully open the biopsy forceps. Therefore, the spacing between the two PMs is 3 to 12 mm and is increased by 0.5 mm when performing FEA. The result is shown in Fig.4(c). As can be seen from the figure, when the spacing between the two PMs increases, the attractive force will gradually decrease. The simulation value of the attractive force can be used to estimate the amount of clamping force generated by the biopsy forceps.

C. Kinematics and Force Analysis of Biopsy Tools

Fig.5(a)(b) shows the movement of the biopsy forceps as it gradually opens under the action of repulsive force. Where AB represents the round shaft, BC represents the connecting rod, CE represents the blade. All the parts are connected with pins and point D is fixed. θ_1 is the angle between the round shaft and the connecting rod, θ_2 is the angle between the connecting rod and the blade, and θ_3 represents half of the open angle of the biopsy forceps. The lengths of L_1, L_2 and L_3 are known. F_R is the repulsive force produced by MTS. d_1 is the displacement when the round shaft advances. When the biopsy forceps are in the state shown in Fig. 5(a). The value of θ_1, θ_2 are very small and can be ignored. Therefore, the length of BD can be expressed as follow:

$$BD = L_1 + L_2 \tag{2}$$

As shown in Fig.5(b), when point B moves under the action of repulsive force F_R, the distance $B^{'}D$ can be calculated as follows:

$$B^{'}D = L_1 + L_2 - d_1 \tag{3}$$

After knowing the value of L_1, L_2 and $B^{'}D$, according to the cosine theorem, the cosine of angle θ_3 is easy to obtain:

$$\cos\theta_3 = \frac{L_2^2 + \left(B^{'}D\right)^2 - L_1^2}{2L_2\left(B^{'}D\right)} \tag{4}$$

Combined with Equation (3) and Equation (4), the relationship between the displacement d_1 and the angle θ_3 can be expressed by the following formula:

$$\theta_3 = \arccos\left[\frac{2L_2^2 + 2L_1L_2 + d_1^2 - 2\left(L_1 + L_2\right)d_1}{2L_2\left(L_1 + L_2 - d_1\right)}\right] \tag{5}$$

Fig.5(c) shows the force diagram of biopsy forceps under the action of attractive force F_A. F_C is the clamping force at point E. When calculating the clamping force F_C, the friction of the pin connection can be neglected, and the calculation formula of F_C can be obtained from moment balance as follows:

$$F_C = \frac{F_A \sin\theta_2 L_2}{2L_3 \cos\theta_1} \tag{6}$$

where L_2 represents the length of power arm, and L_3 represents the length of resisting arm.

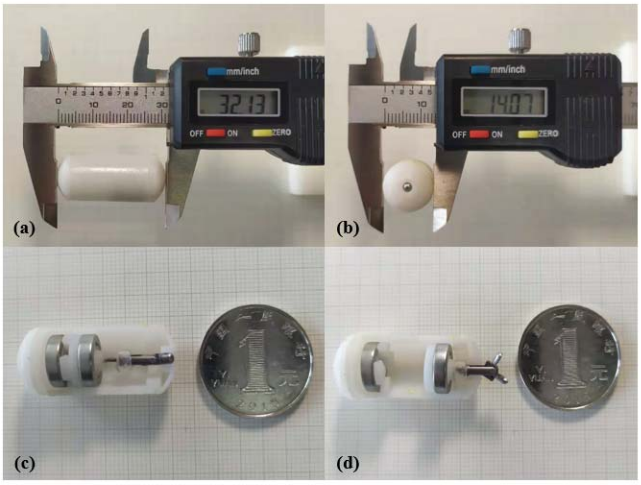

Fig. 6. Full size prototype of the proposed capsule robot. (a) The length of the capsule. (b) The diameter of the capsule. (c) The interior of the capsule in the attraction state. (d) The interior of the capsule in the open state.

D. Capsule Fabrication

The structural design of the proposed capsule robot was completed using Creo 6.0 software. For now, we just need to verify the feasibility of the biopsy mechanism design. Therefore, this version of capsule does not have LEDs, cameras and signal transmission modules installed. Biopsy forceps and magnets can be purchased directly. The rest parts are manufactured using a high-resolution 3D printer, and the material for 3D printing is photosensitive resin. The design size of our capsule is 14mm in diameter and 32mm in length. As shown in Fig.6(a)(b), the actual size is 14.07 mm in diameter and 32.13 mm in length, and the manufacturing error is within an acceptable range. Fig6.(c)(d) shows the internal details of our capsule in two different states.

III. Experimental Assessment

A. Magnetic Driving System

As shown in Fig7(a), we built a magnetic driving system to verify the feasibility of the capsule structure design. The system consists of four electromagnetic coils with magnetic cores, One pair along the x-axis and one pair along the y-axis. Each coil has 900 turns and is powered by the IT6431 high-precision DC bipolar power supply, the voltage regulation range is $\pm$ 15V and the current regulation range is $\pm$ 10A. When electrified, each coil can generate a gradient magnetic field separately. Gradient magnetic field can be used for the propulsion of our capsule, so that the capsule can be moved in the direction of the gradient magnetic field. In addition to the gradient magnetic field, the system can also generate a uniform magnetic field. For instance, when the two coils on the x-axis are respectively supplied with equivalent currents in opposite directions, a uniform magnetic field is generated within the vicinity of the midpoint between the two coils. The uniform magnetic field can be used to remotely activate the biopsy module.

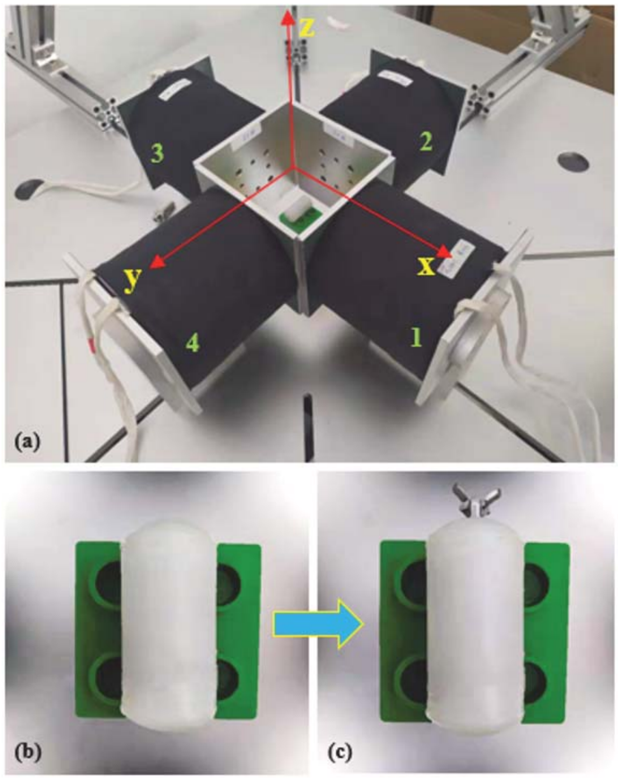

Fig. 7. Schematic of the experiment. (a) Magnetic driving system for the proposed capsule. (b) No uniform magnetic field is applied. (c) After applying a uniform magnetic field, the biopsy forceps of the capsule extended.

B. Experimental Process and Results

In this section, we will test the feasibility of our capsule's biopsy module. As illustrate in Fig7(a), we place the capsule in the middle of the square area enclosed by the four coils. The biopsy forceps extends in the same direction as the positive direction of the y-axis. Therefore, in order to open the biopsy module, we need to generate a uniform magnetic field along the x-axis. Fig7(b)(c) shows the results of the experiment. With the increase of the current, the biopsy forceps successfully extended. After the power is turned off, the biopsy forceps can also be retracted into the capsule immediately. Accordingly, we confirmed that the biopsy module of the capsule is working properly. This result opens up possibilities for further ex-vivo biopsy experiments.

To test the active locomotion of our capsule robot, we placed it in silicone fluid of 350 CS. The role of silicone fluid is to reduce the friction between capsule robot and the lower surface. It also provides a certain viscous resistance to make the movement of the capsule robot more stable. Firstly, we tested the rotational motion of the capsule robot. After the two PMs are aligned. A rotating uniform magnetic field can be generated by applying a sinusoidal current and a cosine current to the two pairs of coils respectively [14]. Then the capsule robot will rotate as the magnetic field rotates. The experimental results are shown in Fig8(a). Secondly, we tested the rolling motion of the capsule robot. We flipped the whole magnetic driving system 90 degrees so that the y-z plane was parallel to the ground. Then we placed the capsule robot on the y-z plane, and the biopsy forceps extends in the same direction as the positive direction of the z-axis. Similarly, we make the magnetic driving system generate a rotating uniform magnetic field so that the capsule can roll forward. The experimental results are shown in Fig8(b).

IV. Conclusions

In this paper, a novel wireless capsule robot with targeting biopsy function was proposed. The MTS mechanism consisting of two permanent magnets was introduced and used as a triggered actuator. A uniform magnetic field generated by the external magnetic driving system can trigger MTS remotely. After being triggered, the repulsive force generated by the MTS can be used as a driving force to push the biopsy tool out. In order to verify the feasibility of the biopsy mechanism design of our capsule, a prototype with dimension of 14 mm in diameter and 32 mm in length was designed and fabricated. With this prototype, we conducted an experiment and the biopsy module of the capsule worked well. We have also successfully achieved the rotational and rolling motion of the capsule robot in a 2-D plane. In the future work, we will conduct an ex-vivo biopsy experiments in porcine stomach to verify whether the biopsy module can successfully collect enough lesion tissues(1$\sim$5mm^3) [15] [16].

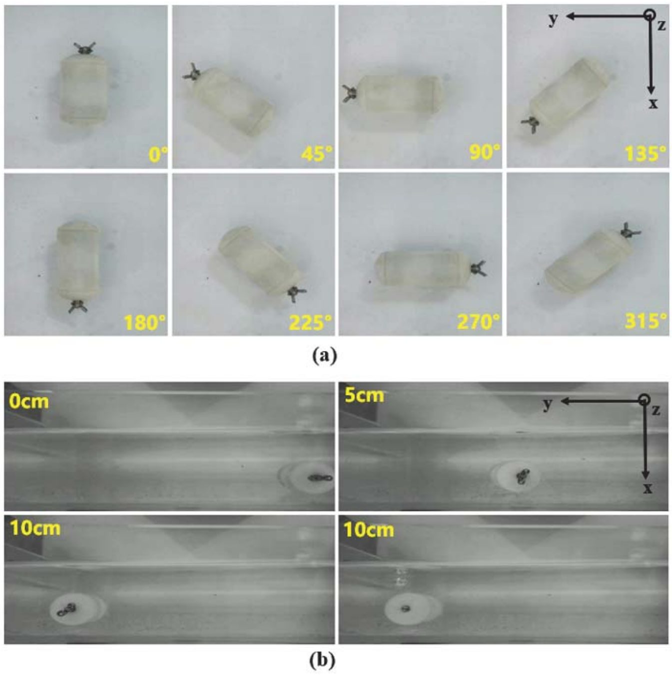

Fig. 8. The movement of our capsule robot in silicone fluid. (a) The capsule robot rotates under the action of a rotating magnetic field(x-y represents the horizontal plane). (b) The capsule robot rolls forward 10cm along the y axis (y-z represents the horizontal plane).

References

[1] Iddan, G., Meron, G., Glukhovsky, A., & Swain, P. (2000). Wireless capsule endoscopy. Nature, 405(6785), 417.
[2] Pan, X., Ma, T., Li, P., Jiang, X., &Song, S. (2018, October). A novel intestinal microcapsule endoscope robot with biopsy function. In 2018 IEEE International Conference on Cyborg and Bionic Systems (CBS) (pp. 308-312). IEEE.
[3] Park, S., Koo, K. I., Bang, S. M., Park, J. Y., & Song, S. Y. (2008). A novel microactuator for microbiopsy in capsular endoscopes. Journal of Micromechanics and Microengineering, 18(2), 025032.
[4] Du, X., Chan, K. F., Xia, X., Chiu, P. W. Y., & Zhang, L. (2018, October). A Magnetically-Triggered Soft Capsule for On-Demand Mucus Collection. In 2018 IEEE International Conference on Cyborg and Bionic Systems (CBS) (pp. 250-254). IEEE.
[5] Simi, M., Gerboni, G., Menciassi, A., & Valdastri, P. (2013). Magnetic torsion spring mechanism for a wireless biopsy capsule. Journal of Medical Devices, 7(4), 041009.
[6] Son, D., Gilbert, H., & Sitti, M. (2019). Magnetically Actuated Soft Capsule Endoscope for Fine-Needle Biopsy. Soft robotics.
[7] Hoang, M. C., Le, V. H., Kim, J., Choi, E., Kang, B., Park, J. O., & Kim, C. S. (2019). Untethered Robotic Motion and Rotating Blade Mechanism for Actively Locomotive Biopsy Capsule Endoscope. IEEE Access, 7, 93364-93374.
[8] Lee, C., Choi, H., Go, G., Jeong, S., Ko, S. Y., Park, J. O., & Park, S. (2014). Active locomotive intestinal capsule endoscope (ALICE) system: A prospective feasibility study. IEEE/ASME Transactions on Mechatronics, 20(5), 2067-2074.
[9] Zhou, H., Alici, G., & Munoz, F. (2016). A magnetically actuated anchoring system for a wireless endoscopic capsule. Biomedical microdevices, 18(6), 102.
[10] Zhou, H., & Alici, G. (2019). A novel magnetic anchoring system for wireless capsule endoscopes operating within the gastrointestinal tract. IEEE/ASME Transactions on Mechatronics.
[11] Le, V. H., Lee, C., Go, G., Park, J. O., & Park, S. (2017). Miniaturized biopsy module using gripper tool for active locomotive capsule endoscope. Mechatronics, 44, 52-59.
[12] Slawinski, P. R., Obstein, K. L., & Valdastri, P. (2015). Emerging issues and future developments in capsule endoscopy. Techniques in Gastrointestinal Endoscopy, 17(1), 40-46.
[13] Montague, R., Bingham, C., & Atallah, K. (2011). Servo control of magnetic gears. IEEE/Asme Transactions on Mechatronics, 17(2), 269-278.
[14] Jang, G. B., Jeon, S., Nam, J., Lee, W., & Jang, G. (2015). A Spiral Microrobot Performing Navigating Linear and Drilling Motions by Magnetic Gradient and Rotating Uniform Magnetic Field for Applications in Unclogging Blocked Human Blood Vessels. IEEE Transactions on Magnetics, 51(11), 1-4.
[15] Catassi, C., & Fasano, A. (2010). Celiac disease diagnosis: simple rules are better than complicated algorithms. The American journal of medicine, 123(8), 691-693.
[16] Hopper, A. D., Cross, S. S., & Sanders, D. S. (2008). Patchy villous atrophy in adult patients with suspected gluten-sensitive enteropathy: is a multiple duodenal biopsy strategy appropriate?. Endoscopy, 40(03), 219-224.